Joint Coupling for Human Shoulder Complex

Jingzhou (James) Yang[1], Xuemei Feng[2], Joo H. Kim[3], Yujiang Xiang[3], and Sudhakar Rajulu[4]

[1] Department of Mechanical Engineering
Texas Tech University, Lubbock, TX79409, USA
[2] Wuhan University of Technology, Wuhan, Hubei, China
[3] Center for Computer-Aided Design, University of Iowa, Iowa City, USA
[4] NASA Johnson Space Center, Houston, TX77058, USA
james.yang@ttu.edu

Abstract. In this paper, we present an inverse kinamtics method to determining human shoulder joint motion coupling relationship based on experimental data in the literature. The joint coupling relationship is available in the literature, but it is an Euler–angle-based relationship. This work focuses on transferring Euler-angle-based coupling equations into a relationship based on the Denavit-Hartenberg (DH) method. We use analytical inverse kinematics to achieve the transferring. Euler angles are obtained for static positions with intervals of 15 degrees, and the elevation angle of the arm varied between 0 and 120 degrees. For a specific posture, we can choose points on clavicle, scapula, and humerus and represent the end-effector positions based on Euler angles or DH method. For both systems, the end-effectors have the same Cartesian positions. Solving these equations related to end-effector positions yields DH joint angles for that posture. The new joint motion coupling relationship is obtained by polynomial and cosine fitting of the DH joint angles for all different postures.

Keywords: Keywords: Human shoulder; joint motion coupling; joint limit coupling; shoulder rhythm; Euler angles; DH method.

1 Introduction

Human shoulder complex consists of three bones—the clavicle, scapula, and humerus—and more than 20 muscles. The shoulder complex model is the key to correctly simulating human posture and motion. So far, various kinds of kinematics shoulder models are available and are based on various methods. Among those methods, the Denavit-Hartenberg (DH) method is an effective way to control the digital human movement in the virtual simulation field [18]. In the literature, two categories can be found: open-loop chain systems and closed-loop chain systems [3]. There are different types of models within each category. Also, we proposed a closed-loop chain model [4] for the shoulder complex. This model is high–fidelity, and the digital human system operates in real-time.

To correctly model the movement of the human shoulder complex, a high-fidelity kinematic model is not enough; a phenomenon called shoulder rhythm should be considered. Shoulder rhythm includes joint motion coupling and joint limit coupling.

V.G. Duffy (Ed.): Digital Human Modeling, HCII 2009, LNCS 5620, pp. 72–81, 2009.

Joint limit coupling has been investigated by Lenarcic and Umek [13], Klopcar and Lenarcic [10, 11], Klopcar et al., [12], and Lenarcic and Klopcar [14]. Joint motion coupling was obtained using an experiment [8]; however, this relationship is Euler-based, and we cannot use it in the DH-based digital human environment.

In previous work [4], we proposed one method for transferring Euler-based coupling equations into DH-based relationships based on a shoulder model in Virtools®. That method is tedious and depends on the model in Virtools. This paper presents an analytical inverse kinematics based method for mapping between the two systems. We first summarize the new proposed shoulder complex model. Next, we briefly discuss the joint coupling equations depicted in Euler angle. For an end-effector position, we can define it as a function of Euler angles or DH joint angles. Solving this analytical inverse kinematic problem, we can obtain a set of DH joint angles. Repeating this procedure for all end-effector positions yields different sets of data. Then these separate data are fitted into a set of functional equations accordingly. Finally, we plot the coupling equations based on polynomial and cosine fitting and compare the different fitting results.

2 Shoulder Kinematic Model

In previous section, we summarized that there are open-loop chain and closed-chain systems. Within the first one, there are five different models (the 5-DOF models I and II, the 6-DOF model, the 7-DOF model, and the 9-DOF model). For a closed-loop chain, several models are also available [3]. We propose a new shoulder model that has 8 DOFs: (1) two revolute joints (q_1, q_2) in the sternoclavicular (SC) joint, denoting clavicle vertical rotation and horizontal rotation; (2) three revolute joints (q_3, q_4, q_5) in the acromioclavicular (AC) joint, denoting rotations in three orthogonal directions of the scapula movement with respect to the local frame; (3) three revolute joints (q_6, q_7, q_8) in the glenohumeral (GH) joint, denoting the movement of the humerus with respect to the local frame.

3 Euler-Angle-Based Joint Coupling Equations

In the past two decades, much research has been done on shoulder complex motion because shoulder pain constitutes a large portion of musculoskeletal disorders in the general population as well as among industrial workers. Shoulder rhythm is one important characteristic to study. Different approaches have been used for this study [1, 2, 6, 7, 8, 16, 17 and 19]. Among these, Hogfors et al. [8] obtained ideal shoulder rhythm solutions. In the study by Hogfors et al. [8], three healthy, right-handed male volunteers (mean age, 24 yr; mean body mass, 70 kg; mean stature 183 cm) were used. They also used numerical evaluation of low roentgen stereophotogrammetric motion pictures of subjects with radiation dense implantations in the bones. Interpolation between measured positions makes it possible to simulate shoulder motions within the normal working range. In the experiment, the orientation angles of the

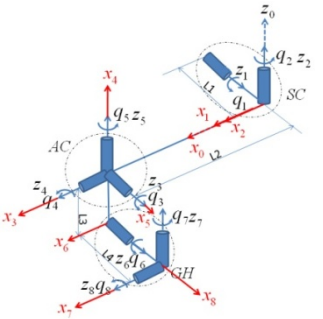

Fig. 1. Shoulder kinematic model

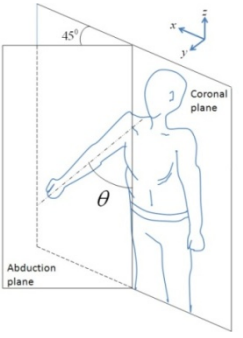

Fig. 2. The elevation angle θ used in the experiment

scapula bone and the clavicle bone were measured when the arm was elevated at the angle θ in the scapular plane, which has 45-degree angle with respect to the coronal plane in Figure 2, where θ varied between 0 and 120 degrees.

Three bones' (clavicle, scapula, and humerus) body-fixed coordinate frames are used to define the orientations of the bones in Figure 3. One global coordinate system is attached on the sternum. The global frame (x, y, z) and the clavicle local frame (x_1, x_2, x_3) have the same origin Ω. The origin of the scapula local frame (ξ_1, ξ_2, ξ_3) is located at point Ω^s. The origin of the humerus frame $(\kappa_1, \kappa_2, \kappa_3)$ is at point Ω^h.

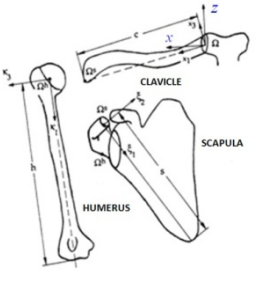

Fig. 3. Coordinate systems for shoulder bones [8]

The Euler angle system α, $-\beta$, and γ shown in Figure 4 was used to depict the movement of the shoulder bones. The transformation matrix is defined by $R_{Eul} = R_X(\gamma)R_Y(-\beta)R_Z(\alpha)$, where

$$R_z(\alpha) = \begin{pmatrix} \cos(\alpha) & -\sin(\alpha) & 0 \\ \sin(\alpha) & \cos(\alpha) & 0 \\ 0 & 0 & 1 \end{pmatrix}, \quad R_y(-\beta) = \begin{pmatrix} \cos(\beta) & 0 & -\sin(\beta) \\ 0 & 1 & 0 \\ \sin(\beta) & 0 & \cos(\beta) \end{pmatrix} \quad R_x(\gamma) = \begin{pmatrix} 1 & 0 & 0 \\ 0 & \cos(\gamma) & -\sin(\gamma) \\ 0 & \sin(\gamma) & \cos(\gamma) \end{pmatrix},$$

while the XYZ frame can be any one of the body-fixed frames for the three bones.

The interpolation results from the experimental data are shown in Eqs. 1-3. The indices *h*, *c,* and *s* for α , $-\beta$, and γ stand for humerus, clavicula, and scapula, respectively. In these equations, α_h and β_h are independent variables. α_h varies from -10^0 to 90^0, and $\beta_h = -90^0 + \theta$ varies within 90-30^0. The angle γ_h in the equations refers to the neutral rotation angle of the upper arm [9]. Humerus:

$$\gamma_h = -45 + \alpha_h[1-(\beta_h+90)/360] + (135-\alpha_h/1.1)\sin(0.5(\beta_h+90)(1+\alpha_h/90)) \quad (1)$$

Clavicle:
$$\begin{cases} \alpha_c = -50 + 30\cos[0.75(\beta_h+90)] \\ \beta_c = 24\{1-\cos[0.75(\beta_h+90)]\}(0.5+\alpha_h/90)+9 \\ \gamma_c = 15\{1-\cos[0.75(\beta_h+90)]\}+3 \end{cases} \quad (2)$$

Scapula:
$$\begin{cases} \alpha_s = 200 + 20\cos[0.75(\beta_h+90)] \\ \beta_s = -140 + 94\cos[0.75(\beta_h+90)(1-\gamma_h/270)] \\ \gamma_s = 82 + 8\cos\{(\alpha_h+10)\sin[0.75(\beta_h+90)]\} \end{cases} \quad (3)$$

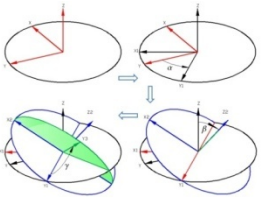

Fig. 4. Euler angles

4 Transferring Joint Coupling Equations from Euler System to DH System

In the above section, we review the coupling equations obtained by experiments in Hogfors et al. [8]. However, it is difficult to use these results directly in digital human models using DH representation instead of Euler angles. This section presents the methodology of transferring these equations from the Euler to the DH system, data generation, data fitting, and discussion about the results from different fitting techniques.

5 Methodology for Transferring the Joint Coupling Equations

The principle of transferring coupling equations from the Euler to the DH system is that the same posture can be represented by different orientation representation systems, i.e., we can represent the same posture with Euler's angles, DH joint angles, Euler parameters, etc. The procedure for transferring the coupling equations shown in Figure 5 entails data generation and equation fitting. Within data generation, there are three steps: (1) selecting key postures based on the Euler system; (3) choosing points on clavicle and humerus AC and GH joint as the end-effectors and form equations

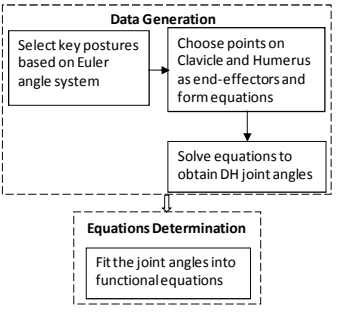

Fig. 5. Methodology for transferring joint coupling equations

(left hand side is the end-effector by Euler system, and right hand side is by DH system); and (3) solving these equations to obtain DH joint angles.

5.1 Data Generation

The global coordinate system is the same for both Euler and DH system. However, DH local frames are different from Euler's frames. Figs. 6 and 7 show the postures corresponding to zero Euler angles and DH angles, respectively.

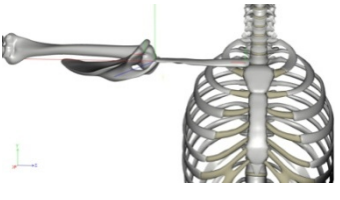

Fig. 6. Zero Euler angles

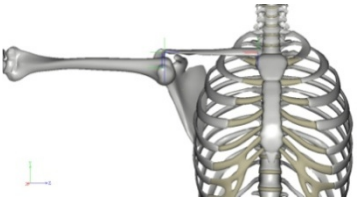

Fig. 7. Zero DH joint angles

In this section, we use one example to illustrate the detailed procedure to determine DH joint angles by analytical inverse kinematics method. When we choose $\alpha_h = 45^o$ and $\beta_h = -45^o$, then, from Eqs. 1-3, all Euler angles are calculated and shown in Table 1. The posture is shown in Figure 8.

Table 1. Euler angles (in degrees)

α_h	β_h	γ_h	α_c	β_c	γ_c	α_s	β_s	γ_s
45	-45	46.6491	-25.0559	13.0447	5.52796	216.629	-56.9405	88.889

Considering AC joint center for both systems, one has the following equations:

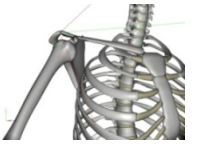

Fig. 8. The shoulder posture when $\alpha_h = 45^0$, $\beta_h = -45^0$

$$\begin{bmatrix} R(\alpha_c, \beta_c, \gamma_c) \cdot \begin{pmatrix} L2 \\ 0 \\ 0 \end{pmatrix} \\ 1 \end{bmatrix} = T_1^0(q_1) \cdot T_2^1(q_2) \cdot \begin{bmatrix} 0 \\ 0 \\ 0 \\ 1 \end{bmatrix} \tag{4}$$

Bringing in all necessary terms in Eq. (4) yields

$$\sin(q_2) = \cos(\beta_c)\sin(\alpha_c) \tag{5}$$

$$\sin(\beta_c) = -\cos(q_2)\sin(q_1) \tag{6}$$

Solving Eqs. (5) and (6), one obtains $\begin{cases} q_1 = 0.2504 \\ q_2 = 2.7163 \end{cases}$ and $\begin{cases} q_1 = -0.2504 \\ q_2 = -0.4253 \end{cases}$ (radians).

One can bring in these solutions into Figure 8 to select the correct solution $\begin{cases} q_1 = -0.2504 \\ q_2 = -0.4253 \end{cases}$.

Choosing GH joint center for both systems, one has

$$\begin{bmatrix} R(\alpha_c, \beta_c, \gamma_c) \cdot \begin{pmatrix} L2 \\ 0 \\ 0 \end{pmatrix} + R(\alpha_s, \beta_s, \gamma_s) \cdot V_{GH}^{Local} \\ 1 \end{bmatrix} = T_1^0(q_1) \cdot T_2^1(q_2) \cdot T_3^2(q_3) \cdot T_4^3(q_4) \cdot T_5^4(q_5) \cdot \begin{bmatrix} 0 \\ 0 \\ L_4 \\ 1 \end{bmatrix} \tag{7}$$

where $V_{GH}^{Local} = \begin{bmatrix} 0.9463 & -0.9463 & 0.4145 \end{bmatrix}^T$ is the GH joint center position corresponding to the scapula fixed frame. Solving the first two equations in Eq.(7), one obtains the following possible solutions: $q_3 = 0.2394$ and $q_4 = -2.9030$, $q_3 = -2.9234$ and $q_4 = -2.6982$, $q_3 = 0.2176$ and $q_4 = -0.4434$, or $q_3 = -2.9022$ and $q_4 = -0.2386$. This is a redundant problem and we bring all possible solutions in Fig. 8 and the correct solution is $q_3 = 0.2176$ and $q_4 = -0.4434$. Solving the third equation in Eq.(7) yields $q_5 = 0.2895$.

Similarly we choose a point on the humerus and have the following equations:

$$\begin{bmatrix} R(\alpha_c,\beta_c,\gamma_c)\cdot\begin{pmatrix} L2 \\ 0 \\ 0 \end{pmatrix} + R(\alpha_s,\beta_s,\gamma_s)\cdot V_{GH}^{Local} + R(\alpha_h,\beta_h,\gamma_h)\cdot V_{HUM}^{Local} \\ 1 \end{bmatrix} = T_8^0(q_1,q_2,q_3,q_4,q_5,q_6,q_7,q_8)\cdot\begin{bmatrix} -1 \\ 0 \\ 1 \\ 1 \end{bmatrix} \quad (8)$$

Solve these equations and check the postures in Fig. 8. The final correct solutions are $q_6 = 0.8612$, $q_7 = 0.6735$, and $q_8 = 0.2528$. Transferring all radians to degrees, one gets the DH joint angles in Table 2.

Table 2. DH joint angles for $\alpha_h = 45^0$, $\beta_h = -45^0$ (in degrees)

q_1	q_2	q_3	q_4	q_5	q_6	q_7	q_8
-14.3469	-24.3679	12.4676	-25.4049	16.5871	49.3427	38.5889	14.4844

Similarly, we can find all DH joint angles for postures with respect to α_h within -10^0 to 90^0 and β_h in -90-30^0.

5.2 Data Fitting

In the above data generation, we find that the joint angle q_8 does not affect the positions and orientation of the clavicle and scapula bones. Therefore, the joint angle q_8 is independent. Joint angles q_1 to q_5 are functions of q_6 and q_7. Based on data from the above section, we can use functional fitting to build up the coupling equations.

There are different functions that can be fitted based on the same set of data. In this study, we choose polynomial, cosine series, and sigmoid functions as the coupling equations. Then we compare these functions to summarize the pros and cons. We use Mathematica® to obtain the fitting functions. The final fitting functions are denoted as follows; the unit is radians.

i. Polynomial functions

$$q_1 = -0.056496q_7^3 - 0.020185q_6^3 - 0.197370q_7^2q_6 + 0.188814q_7q_6^2 + 0.094692q_7^2 - 0.265677q_6^2 - 0.025195q_7q_6 - 0.090610q_7 + 0.587757q_6 - 0.481600$$

$$q_2 = -0.203064q_7^3 - 0.008258q_6^3 + 0.160842q_7^2q_6 + 0.085135q_7q_6^2 + 0.312579q_7^2 - 0.110429q_6^2 - 0.722626q_7q_6 + 0.179235q_7 + 0.753456q_6 - 0.877683$$

$$q_3 = -0.010575q_7^3 + 0.001193q_6^3 + 0.269967q_7^2q_6 - 0.005200q_7q_6^2 - 0.142453q_7^2 + 0.016321q_6^2 - 0.707116q_7q_6 + 0.613453q_7 + 0.440594q_6 - 0.228151$$

$$
\begin{aligned}
q_4 &= 0.015404q_7^3 + 0.008550q_6^3 - 0.308488q_7^2q_6 - 0.099259q_7q_6^2 + 0.375770q_7^2 + \\
&0.134428q_6^2 + 1.122621q_7q_6 - 1.082992q_7 - 1.032156q_6 + 0.400115 \\
q_5 &= 0.019663q_7^3 - 0.004599q_6^3 - 0.047076q_7^2q_6 + 0.061801q_7q_6^2 + 0.021243q_7^2 - \\
&0.086331q_6^2 + 0.095226q_7q_6 - 0.080383q_7 - 0.006919q_6 + 0.328476
\end{aligned} \tag{9}
$$

ii. Fourier series functions

$$
\begin{aligned}
q_1 &= -0.638284 + 0.095253\cos(q_7) - 0.076156\cos(q_6) + 0.002803\sin(q_7) - 0.746368\sin(q_6) - \\
&0.101693\cos(2q_7) + 0.024957\cos(2q_6) - 0.168160\sin(2q_7) + 0.017257\sin(2q_6) + \\
&0.287427\cos(q_7)\cos(q_6) + 1.085183\cos(q_7)\sin(q_6) + 0.045037\sin(q_7)\cos(q_6) + \\
&0.730106\sin(q_7)\sin(q_6) \\
q_2 &= -1.740112 + 0.010163\cos(q_7) + 0.998839\cos(q_6) + 1.212096\sin(q_7) + 0.955282\sin(q_6) + \\
&0.050952\cos(2q_7) - 0.005597\cos(2q_6) + 0.126617\sin(2q_7) + 0.015509\sin(2q_6) - \\
&0.332707\cos(q_7)\cos(q_6) + 0.125642\cos(q_7)\sin(q_6) - 0.973988\sin(q_7)\cos(q_6) - \\
&0.949188\sin(q_7)\sin(q_6) \\
q_3 &= -0.568506 - 0.005966\cos(q_7) + 0.314923\cos(q_6) + 1.087587\sin(q_7) + 0.896371\sin(q_6) + \\
&0.161975\cos(2q_7) + 0.004556\cos(2q_6) + 0.010620\sin(2q_7) + 0.002634\sin(2q_6) - \\
&0.211634\cos(q_7)\cos(q_6) - 0.279816\cos(q_7)\sin(q_6) - 0.319026\sin(q_7)\cos(q_6) - \\
&0.889261\sin(q_7)\sin(q_6) \\
q_4 &= -0.029221 + 0.659483\cos(q_7) - 0.087511\cos(q_6) - 0.453476\sin(q_7) - 0.870285\sin(q_6) - \\
&0.109823\cos(2q_7) - 0.005751\cos(2q_6) - 0.270092\sin(2q_7) + 0.001511\sin(2q_6) - \\
&0.026523\cos(q_7)\cos(q_6) - 0.190386\cos(q_7)\sin(q_6) + 0.103925\sin(q_7)\cos(q_6) + \\
&0.851738\sin(q_7)\sin(q_6) \\
q_5 &= 0.012476 + 0.328949\cos(q_7) - 0.198714\cos(q_6) + 0.335480\sin(q_7) - 0.310143\sin(q_6) - \\
&0.012544\cos(2q_7) + 0.019457\cos(2q_6) - 0.269965\sin(2q_7) + 0.004378\sin(2q_6) + \\
&0.200568\cos(q_7)\cos(q_6) + 0.193417\cos(q_7)\sin(q_6) + 0.158652\sin(q_7)\cos(q_6) + \\
&0.314105\sin(q_7)\sin(q_6)
\end{aligned} \tag{10}
$$

5.3 Discussion

By means of data fitting (or regression), the joint coupling equations in the DH system have been obtained in the above section. However, different fitting functions have their own characteristics, which are summarized in this section.

During the data regression process, two criteria were used. They are coefficient of determination R^2, and maximal absolute residuals. The regression criteria values are presented in Tables 3 and 4. According to statistics theory, a larger R^2 means a better model. Most R^2 in Table 3 are larger than 0.90. The maximal absolute residuals are different for different joints.

Smoothness is another factor to consider when choosing regression functions because human shoulder joints should not have any jerk during motion. From Eqs. 1-3, all functions are smooth.

Joint limits calculated from Eqs. 1-3 are the last factor to be considered for regression functions. Bringing joint limits for q_6 and q_7 into these equations yields a

possible range of motions for the joints q_1 to q_5. These values should be finite and within the given range of motions for each joint.

Based on all the factors mentioned above, the Fourier series functions are the best choice for the final coupling equations in the DH system.

Table 3. Coefficient of Determination R^2

Joint angle	Polyno. function	Trigon. function	Fourier function
q_1	0.964169	0.985975	0.997812
q_2	0.964169	0.985975	0.997812
q_3	0.993352	0.996666	0.998945
q_4	0.991618	0.996725	0.998068
q_5	0.900623	0.911096	0.94599

Table 4. Maximum of absolute residuals in regression equations

Joint angle	Polyno. function	Trigo. function	Fourier function
q_1	0.239784	0.0791158	0.0724016
q_2	0.187342	0.109164	0.0640427
q_3	0.064795	0.0363415	0.0307189
q_4	0.141521	0.0529489	0.0413061
q_5	0.063625	0.0606651	0.0733895

6 Conclusions

This paper presents an analytical inverse kinematics method for transferring coupling equations from the Euler system to the DH system. This method is based on the principle that one posture can be depicted by different rotation representation systems. Key postures from the Euler system were used to obtain the DH joint angles. A shoulder kinematic model was set up in Virtools to eliminate wrong postures, a data fitting technique was implemented, and several types of regression functions were constructed and compared. Fourier series functions are the ideal solutions for these coupling equations based on regression criteria, smoothness, and calculated joint ranges of motion.

The original coupling equations in the Euler system were from experiments, and the hypothesis is that they do not depend on anthropometry. That means these equations generally represent the shoulder rhythm for humans from all percentiles. However, when we transferred these equations in the Euler system to equations in the DH system, specific link lengths were used. If a different set of link lengths were used, then we would get a different set of coupling equations. They would not be significantly different, however, because the shoulder rhythm is similar for humans of all

percentiles [8]. Therefore, these transferred coupling equations in DH system can be approximately used for a human from any percentile.

References

1. Bao, H., Willems, P.Y.: On the kinematic modeling and the parameter estimation of the human shoulder. Journal of Biomechanics 32, 943–950 (1999)
2. Berthonnaud, E., Herzberg, G., Zhao, K.D., An, K.N., Dimnet, J.: Three-dimensional in vivo displacements of the shoulder complex from biplanar radiography. Surg. Radiol. Anat. 27, 214–222 (2005)
3. Feng, X., Yang, J., Abdel-Malek, K.: Survey of Biomechanical Models for Human Shoulder Complex. In: Proceedings of SAE Digital Human Modeling for Design and, Pittsburgh, PA, June 14-16, 2008 (2008a)
4. Feng, X., Yang, J., Abdel-Malek, K.: On the Determination of Joint Coupling for Human Shoulder Complex. In: Proceedings of SAE Digital Human Modeling for Design and, Pittsburgh, PA, June 14-16, 2008 (2008b)
5. de Groot, J.H., Valstar, E.R., Arwert, H.J.: Velocity effects on the scapula-humeral rhythm. Clinical Biomechanics 13, 593–602 (1998)
6. de Groot, J.H., Brand, R.: A three-dimensional regression model of the shoulder rhythm. Clinical Biomechanics 16(9), 735–743 (2001)
7. Herda, L., Urtasun, R., Fua, P., Hanson, A.: Automatic determination of shoulder joint limits using quaternion field boundaries. International Journal of Robotics Research 22(6), 419–436 (2003)
8. Hogfors, C., Peterson, B., Sigholm, G., Herberts, P.: Biomechanical model of the human shoulder joint-II. The shoulder rhythm. J. Biomechanics. 24(8), 699–709 (1991)
9. Karlsson, D., Peterson, B.: Towards a model for force predictions in the human shoulder. J. Biomechanics. 25(2), 189–199 (1992)
10. Klopcar, N., Lenarcic, J.: Kinematic model for determination of human arm reachable workspace. Meccanica 40, 203–219 (2005)
11. Klopcar, N., Lenarcic, J.: Bilateral and unilateral shoulder girdle kinematics during humeral elevation. Clinical Biomechanics 21, S20–S26 (2006)
12. Klopcar, N., Tomsic, M., Lenarcic, J.: A kinematic model of the shoulder complex to evaluate the arm-reachable workspace. Journal of Biomechanics 40, 86–91 (2007)
13. Lenarcic, J., Umek, A.: Simple model of human arm reachable workspace. IEEE Transaction on Systems, Man, and Cybernetics 6, 1239–1246 (1994)
14. Lenarcic, J., Klopcar, N.: Positional kinematics of humanoid arms. Robotica 24, 105–112 (2006)
15. Maurel, W.: 3D modeling of the human upper limb including the biomechanics of joints, muscles and soft tissues. PhD Thesis, Lausanne, EPFL (1995)
16. Moeslund, T.B.: Modeling the human arm. Technical report at Laboratory of Computer Vision and Media Technology, Aalborg University, Denmark (2002)
17. Rundquist, P.J., Anderson, D.D., Guanche, C.A., Ludewig, P.M.: Shoulder kinematics in subjects with frozen shoulder. Arch. Phys Med. Rehabil. 84, 1473–1479 (2003)
18. Sciavicco, L., Siciliano, B.: Modeling and control of robot manipulators. The McGraw-Hill Companies, Inc., New York (1996)
19. Six Dijkstra, W.M.C., Veeger, H.E.J., van der Woude, L.H.V.: Scapular resting orientation and scapula-humeral rhythm in paraplegic and able-bodied male. In: Proceedings of the First Conference of the ISG, pp. 47–51 (1997)